# Inhibition of Dendritic Cell Maturation and Function Is Independent of Heme Oxygenase 1 but Requires the Activation of STAT3



Mir-Farzin Mashreghi, Roman Klemz, Isabela Schmitt Knosalla, Bernhard Gerstmayer, Uwe Janssen, Roland Buelow, Alicja Jozkowicz, Jozef Dulak, Hans-Dieter Volk and Katja Kotsch

*J Immunol* 2008;180;7919-7930



*The Journal of Immunology* is published twice each month by
The American Association of Immunologists, Inc.,
9650 Rockville Pike, Bethesda, MD 20814-3994.

Print ISSN: 0022-1767 Online ISSN: 1550-6606.

# Inhibition of Dendritic Cell Maturation and Function Is Independent of Heme Oxygenase 1 but Requires the Activation of STAT3[1]

**Mir-Farzin Mashreghi,* Roman Klemz,* Isabela Schmitt Knosalla,* Bernhard Gerstmayer,‡ Uwe Janssen,‡ Roland Buelow,§ Alicja Jozkowicz,¶ Jozef Dulak,¶ Hans-Dieter Volk,*† and Katja Kotsch[2]***

**The induction of heme oxygenase 1 (HO-1) by a single treatment with cobalt protoporphyrin (CoPPIX) protects against inflammatory liver failure and ischemia reperfusion injury after allotransplantation. In this context, the HO-1-mediated inhibition of donor-derived dendritic cell maturation and migration is discussed as one of the key events of graft protection. To investigate the poorly understood mechanism of CoPPIX-induced HO-1 activity in more detail, we performed gene expression analysis in murine liver, revealing the up-regulation of *STAT3* after CoPPIX treatment. By using wild-type and HO-1-deficient dendritic cells we demonstrated that LPS-induced maturation is dependent on STAT3 phosphorylation and independent of HO-1 activity. In summary, our observations revise our understanding of the anti-inflammatory properties of HO-1 and highlight the immunomodulatory capacity of STAT3, which might be of further interest for targeting undesired immune responses, including ischemia reperfusion injury.** *The Journal of Immunology,* **2008, 180: 7919–7930.**

Dendritic cells (DCs)[3] are potent APCs that play a major role in the initiation and modulation of immune responses (1). Most peripheral tissues harbor immature DCs capable of capturing and processing Ags. Upon activation, DCs migrate to secondary lymphoid tissues where they undergo final maturation (1–3). This is the case early after solid organ transplantation, when donor-derived DCs are the main mediators for acute rejection because they stimulate direct T cell alloresponses against the graft (4–6). The importance of DCs shifting the immune response toward either tolerance or acute rejection has been further demonstrated, because the administration of liver-derived immature DCs before transplantation induced donor-specific hyporesponsiveness (7) whereas an increase in DC maturation and number resulted in acute rejection of the liver allograft (8, 9).

Because inflammatory changes within the graft, including ischemia reperfusion (I/R) injury, initiate the maturation of donor DCs in vivo (10), one aim of targeting inflammation in transplant medicine is to prevent donor DC maturation. Evidence that the cytoprotective enzyme heme oxygenase 1 (HO-1) modulates DCs was recently provided by the demonstration that an induction of HO-1 by the metalloporphyrin cobalt-protoporphyrin IX (CoPPIX) could inhibit LPS-induced bone-marrow-derived DCs (BMDCs), whereas tin-protoporphyrin (SnPPIX), which is known to block HO-1 activity (11), showed no effect on the maturation process (12, 13). HO-1 catabolizes heme into three byproducts, carbon monoxide (CO), iron, and biliverdin (14), and biliverdin is further converted to bilirubin through biliverdin reductase. HO-1 is classified as heat shock protein 32 (HSP32) and is induced in response to various stimuli such as hypoxia, endotoxins, heat shock, reactive oxygen species (ROS), or ischemia, acting as a cytoprotective protein (15). The observed inhibition of phenotypic DC maturation as a consequence of HO-1 induction (12) might be one of the major mechanisms explaining the observation that the application of CoPPIX in organ donors could lead to prolonged allogeneic graft survival in kidney (16, 17), heart (18), and bone marrow transplantation (19). Additionally it has been demonstrated that treatment with CoPPIX to induce HO-1 ameliorated I/R injury (20, 21) and that a single donor treatment with methylene chloride (MC) to induce CO ameliorated chronic allograft nephropathy, as reflected in the reduced number of donor-derived DCs (22). Recently, we demonstrated that CoPPIX-mediated induction of HO-1 in rat BMDCs matured with LPS resulted in reduced mRNA expression of MHC class II and costimulatory molecules. Similar results were obtained in an experimental model of kidney transplantation. The CoPPIX treatment of organ donors for HO-1 induction 24 h before organ harvesting led to decreased levels of MHC class II expression and costimulatory molecules in the recipient's spleen, suggesting diminished migration and activation of donor-derived DCs (23).

*Institute of Medical Immunology and †Berlin-Brandenburg Center of Regenerative Therapies, Charité Universitätsmedizin Berlin, Berlin, Germany; ‡Miltenyi Biotec GmbH, Bergisch Gladbach, Germany; §Therapeutic Human Polyclonals Inc., Mountain View, CA 94043; and ¶Department of Medical Biotechnology, Faculty of Biochemistry, Biophysics and Biotechnology, Jagiellonian University, Krakow, Poland

Received for publication January 23, 2008. Accepted for publication April 14, 2008.

The costs of publication of this article were defrayed in part by the payment of page charges. This article must therefore be hereby marked *advertisement* in accordance with 18 U.S.C. Section 1734 solely to indicate this fact.

[1] M.-F.M. is a recipient of the Charité Graduation grant and the GlaxoSmithKline travel grant. The study was supported by grant N301 08032/3156 from the Ministry of Science and Higher Education and by the European Vascular Genomics Network contract LSHM-CT 2003-503254 (to J.D.). A.J. is the International Senior Research Fellow of Wellcome Trust.

[2] Address correspondence and reprint requests to Dr. Katja Kotsch, Institute of Medical Immunology, Charité Universitätsmedizin Berlin, Campus Mitte, Charitéplatz 1, D-10117, Berlin, Germany. E-mail address: katja.kotsch@charite.de

[3] Abbreviations used in this paper: DC, dendritic cell; BCL3, B cell lymphoma 3; BMDC, bone marrow-derived DC; CO, carbon monoxide; CoPPIX, cobalt-protoporphyrin IX; Ct, cycle threshold; HO-1 heme oxygenase 1; HPRT, hypoxanthine guanine phosphoribosyltransferase; I/R, ischemia reperfusion; MC, methylene chloride; n.s. nonsilencing; PDL-1, programmed death ligand 1; ROS, reactive oxygen species; SnPPIX, tin-protoporphyrin IX; siHO-1, siRNA against HO-1; siRNA, small interfering RNA; siSTAT3, siRNA against STAT3; SOCS3, suppressor of cytokine signaling 3.

Against the background of the immunomodulatory capacity of CoPPIX-induced HO-1 overexpression, we aimed to uncover the molecular mechanisms downstream of HO-1. To investigate potential candidate genes for CoPPIX-mediated HO-1 induction and its byproduct, CO, we performed gene expression analysis of murine whole liver tissue by using customized cDNA microarrays after the treatment of mice with CoPPIX, MC for CO induction, and CO exposure. Remarkably, STAT3 was shown to be induced shortly after treatment with CoPPIX. As it has been shown that STAT3 activation is able to block the maturation of BMDCs (24), we investigated whether HO-1 (12) or STAT3 activation is responsible for the CoPPIX-mediated suppression of DC maturation after LPS treatment. In summary, our data illustrate that this inhibitory effect is associated with an activation of STAT3 and could not be attributed to the activity of HO-1.

## Materials and Methods

### *Animals*

Animal care and experimental procedures were performed under pathogen-free conditions in accordance with established institutional guidance and approved protocols from the Animal Care Facility of Charité Universitätsmedizin, Berlin, Germany. Male BALB/c and C57BL/6 mice at the age of 8 wk were purchased from Harlan Winkelmann. HO-$1^{-/-}$ knockout and wild-type C57BL/6 × FVB (8–10 wk) mice (25) were bred in the Animal Facility of the Department of Medical Biotechnology, Jagiellonian University (Kraków, Poland).

### *In vivo treatment*

For the analysis of gene expression profiles in vivo, C57BL/6 mice were treated either with 5 mg/kg CoPPIX i.p., 50 mg/kg MC per os, or 500 ppm CO for 6 or 24 h (three animals in each group). Untreated C57BL/6 mice were used as controls ($n = 9$). After 6 or 24 h of treatment, animals were sacrificed and whole livers were recovered for analysis.

### *cDNA array production*

A customized PIQOR cDNA microarray (Miltenyi Biotec) spotted with 792 immune-related murine and 27 rat-specific cDNAs was used for analysis. Array production was done as previously described (26, 27). Briefly, defined 200- to 400-bp fragments of selected cDNAs were generated by RT-PCR (SuperScript II; Invitrogen), cloned into pGEM-T vector (Promega), and sequence verified. Amplified inserts (*Taq* PCR master mix; Qiagen) were purified (QIAquick 96 PCR BioRobot kit; Qiagen), checked on an agarose gel, and spotted four times (0.2 ng) on pretreated glass slides with a noncontact, piezo-based spotting device.

### *Isolation of total RNA, labeling, and hybridization*

Whole liver tissues were disrupted with an Ultra-Turrax homogenizer (Janke & Kunkel). Total RNA was extracted from whole organs using the NucleoSpin RNA L kit (Macherey-Nagel). Sample quality and quantity were assessed with an Agilent 2100 Bioanalyzer (Agilent Technologies). All samples possessed 18S and 28S rRNA peaks with no RNA degradation. mRNA isolation and fluorescent labeling of the probes were performed as previously described (26, 27). Briefly, 100 μg of total RNA was combined with a control RNA consisting of an in vitro transcribed *Escherichia coli* genomic DNA fragment carrying a 30-nt poly(A)$^+$ tail, and the mRNA was isolated (Oligotex mRNA mini kit; Qiagen). The resulting mRNA was diluted to 17 μl and combined with 2 μl of a second control RNA, a mixture of three different transcripts. The mRNA was then reverse transcribed by adding it to a mix consisting of 8 μl of 5× first strand buffer (Invitrogen), 2 μl of primer mix (oligo(dT) and randomers), 2 μl of low-C dNTPs (10 mM dATP, 10 mM dGTP, 10 mM dTTP; and 4 mM dCTP), 2 μl of FluoroLink Cy3/5-dCTP (Amersham Biosciences), 4 μl of 0.1 M DTT, and 1 μl of RNasin (20–40 U) (Promega). SuperScript II reverse transcriptase (200 U; Invitrogen) was added and incubated at 42°C for 30 min followed by the addition of a further 1 μl of SuperScript II reverse transcriptase, and incubation under the same conditions detailed above was conducted. RNaseH (0.5 μl; Invitrogen) was added and incubated at 37°C for 20 min to hydrolyze RNA. Cy3- and Cy5-labeled samples were combined and cleaned up using QIAquick (Qiagen). Eluents were diluted to a volume of 50 μl. Fifty microliters of 2× hybridization solution (Miltenyi Biotec) prewarmed to 42°C were added. Hybridization was performed according to the manufacturer's guidelines (Miltenyi Biotec) using a GeneTAC hybridization station (PerkinElmer). Slides were fixed in the GeneTAC hybridization station. One hundred microliters of prehybridization solution were added and slides were prehybridized at 65°C for 30 min. Then 100 μl of purified, mixed Cy3- and Cy5-labeled probes in 2× hybridization solution was pipetted onto the slides, thereby displacing the prehybridization solution. Hybridization was then performed for 14 h at 65°C, followed by four washing steps conducted at 50°C following the manufacturer's instructions (Miltenyi Biotec). RNA from control livers was labeled with Cy3-dCTP, and RNA from treated samples was labeled with Cy5-dCTP.

### *Data analysis*

In total, 42 cDNA microarray experiments were performed. Image capture and signal quantification of hybridized PIQOR cDNA microarrays were done with the ScanArray3000 (GSI Lumonics) and ImaGene software version 4.1 (BioDiscovery). For each spot, the local signal was measured inside a fixed circle 350 μm in diameter, and the background was measured outside the circle within specified rings 40 μm distant to the signal and 40 μm wide. Signal and background were taken to be the average of pixels between defined low and high percentages of maximum intensity, with percentage of parameter settings for low/high being 0/97% for signal and 0/80% for background. Local background was subtracted from the signal to give the net signal intensity and the ratio of Cy5/Cy3. The ratios were normalized to the median of all ratios by using only those spots for which the fluorescent intensity in one of the two channels was two times the negative control. Subsequently, the mean of the ratios of four corresponding spots representing the same cDNA was computed. The negative control for each array was computed as the mean of the signal intensity of four spots representing herring sperm and four spots representing spotting buffer only. Only genes displaying a net signal intensity 2-fold higher in the control or treatment sample than in the negative control were used for further analysis. For linear scaling, ratios with values $<1$ were treated in the following way: (1/ratio) × −1. Therefore, −1 and + 1 values were considered as equal. The data discussed in this publication have been deposited in the Gene Expression Omnibus (GEO; www.ncbi.nlm.nih.gov/geo/) of the National Center for Biotechnology Information and are accessible through GEO Series accession no. GSE8452.

### *Quantitative real-time RT-PCR*

Real-time RT-PCR was performed as described elsewhere (28). The expression of selected genes was analyzed by real-time PCR using the ABI PRISM 7500 sequence detection system (TaqMan; PerkinElmer Biosystems). We designed amplification primers and probes for STAT3, suppressor of cytokine signaling 3 (SOCS3), HO-1, TNF-α, IL-6, IL-10, IL-12p40, programmed death ligand-1 (PDL-1), IFN-γ, and hypoxanthine guanine phosphoribosyltransferase (HPRT) to span the exon borders to exclude cross-reactivity with genomic DNA using Primer Express software 2.0 (Applied Biosystems) (Table I). Gene expression analysis of CD80, CD86, MHC class II, ICAM-1, and B cell lymphoma 3 (BCL3) was performed using TaqMan gene expression assays (Applied Biosystems) according to the manufacturer's instructions. SYBR Green PCR was performed in a final volume of 25 μl containing 1 μl of cDNA, 12.5 μl of Brilliant SYBR Green QPCR master mix (Stratagene), 6 μl of primer mix, and 6.5 μl of distilled water. Specific gene expression was normalized to the housekeeping gene β-actin or HPRT by using the formula $2^{-\Delta Ct}$ (where Ct is threshold cycle), which also showed no regulation in the microarray experiments. The result for the relative gene expression was calculated by the $2^{-\Delta\Delta Ct}$ method. The mean Ct values for the genes of interest and the housekeeping gene were calculated from double determinations. Samples were considered negative if the Ct values exceeded 40 cycles.

### *Cell preparation*

Murine BMDCs were generated as previously described (29). In brief, $7.5 \times 10^5$ or $7.5 \times 10^4$ bone marrow cells were cultured in either 24-well or 96-well plates (BD Biosciences) with RPMI 1640 supplemented with 10% FBS, 1% penicillin-streptomycin (PAA Laboratories), and 10 ng/ml recombinant murine GM-CSF. Cultures were fed every 2 days with fresh medium containing recombinant murine GM-CSF. On day 7, adherent immature BMDCs (purity ≥ 90% CD11c$^+$) were used for additional experiments. Murine CD4$^+$ T cells were isolated from spleen and enriched using CD4$^+$ MACS beads (Miltenyi Biotec) according to the manufacturer's instructions. Purity of isolated cells was routinely ≥97%.

### *siRNA design*

Small interfering RNA (siRNA) against STAT3 was designed using the siRNA Selection Program at the Whitehead Institute for Biomedical Research, Cambridge, MA (30). The sense and antisense strands of murine

Table I. *Sequences of amplification primers and probes for real-time RT-PCR*

| Gene | Amplification Primers (5′ to 3′) |
|---|---|
| STAT3 | |
| Sense | GAGAGCCAGGAGCACCCC |
| Antisense | TCACACAGATGAACTTGGTCTTCAG |
| Probe | CCGACCCAGGTAGTGCTGCCCC |
| SOCS3 | |
| Sense | AGTAGAGCTGGCAGGACCTGG |
| Antisense | CGCTTGTCAAAGGTATTGTCCC |
| | SYBR Green |
| HO-1 | |
| Sense | CAGAAGAGGCTAAGACCGCCTT |
| Antisense | TCTGGTCTTTGTGTTCCTCTGTCA |
| Probe | TGCTCAACATTGAGCTGTTTGAGGAGCTG |
| TNF-α | |
| Sense | TCGAGTGACAAGCCCGTAGC |
| Antisense | CTCAGCCACTCCAGCTGCTC |
| Probe | CGTCGTAGCAAACCACCAAGCGGA |
| HPRT | |
| Sense | ATCATTATGCCGAGGATTTGGAA |
| Antisense | TTGAGCACACAGAGGGCCA |
| Probe | TGGACAGGACTGAAAGACTTGCTCGAGATG |
| | SYBR Green |
| IFN-γ | |
| Sense | AGCAACAGCAAGGCGAAAAA |
| Antisense | AGCTCATTGAATGCTTGGCG |
| Probe | ATTGCCAAGTTTGAGGTCAACAACCCACA |
| IL-10 | |
| Sense | GAAGACCCTCAGGATGCGG |
| Antisense | CCTGCTCCACTGCCTTGCT |
| Probe | CGCTGTCATCGATTTCTCCCCTGTGA |
| IL-12 | |
| Sense | GAACTACAGCACCAGCTTCTTCATC |
| Antisense | CTTCAAAGGTTTCACCTGCAGG |
| Probe | ACATCATCAAACCGGACCCACCCAA |
| IL-6 | |
| Sense | TCCAGAAACCGCTATGAAGTTCC |
| Antisense | GTCACCAGCATCAGTCCCAAG |
| Probe | CTCTGCAAGAGACTTCCATCCAGTTGCCT |
| PLD-1 | |
| Sense | ATCACAGCCAGGGCAAAACC |
| Antisense | CCTGTTCTGTGGAGGATGTGTTG |
| | SYBR Green |

STAT3 siRNA were 5′-CCUCCAGGACGACUUUGAU-3′ (sense) and 5′-AUCAAAGUCGUCCUGGAGG-3′ (antisense). The applied HO-1 siRNA was 5′-GCCACACAGCACUAUGUAA-3′ (sense) and 5′-UUACAUAGUGCUGUGUGGC-3′ (antisense) as already described (31). The nonsilencing (n.s.) siRNA as negative control was 5′-UUCUCCGAACGUGUCACGU-3′ (sense) and 5′-ACGUGACACGUUCGGAGAA-3′ (antisense). All lyophilized, 2′-deprotected, desalted, and purified siRNA duplexes were prepared according to the manufacturer's instructions (Qiagen).

### *Transfection of immature BMDCs with siRNA*

Immature BMDCs were transfected at day 7 with HiPerFect transfection reagent (Qiagen) according to the manufacturer's instructions. Briefly, immature BMDCs seeded in 24-well plates were fed with 500 μl of RPMI 1640 supplemented with 10% FBS and 1% penicillin-streptomycin (PAA Laboratories). siRNAs were diluted in a final volume of 100 μl of OptiMEM medium (Invitrogen), 6 μl of HiPerFect reagent was added, and the mixture was incubated for 15 min for complex formation. The transfection mixture was added dropwise onto the immature BMDC culture. The cells were incubated at 37°C with 5% $CO_2$ for 16 h until treatment. The transfection rate was routinely ≥80% and the viability of the BMDCs was not influenced by this method (data not shown).

### *Isolation of total RNA from BMDCs and cDNA synthesis*

Isolation of total RNA from BMDCs was performed using the Absolutely RNA Miniprep kit (Stratagene) and reverse transcribed into cDNA by the murine leukemia reverse transcriptase (Invitrogen) according to the manufacturer's instructions.

### *Treatment of BMDCs with cucurbitacin I, metalloprotoporphyrins, IL-10, and LPS*

On day 8, murine immature BMDCs (including DCs transfected with siRNA) were treated for either 2 or 6 h with 50 μM CoPPIX, SnPPIX (Frontier Scientific), or sodium hydroxide (0.04 M NaOH (pH 7.4)). In addition BMDCs were pretreated with or without 50 ng/ml recombinant murine IL-10 (NatuTec) for either 6 or 18 h. Cells were then washed twice and cultured for a further 2 or 6 h. For STAT3 inhibitor experiments, immature BMDCs were pretreated for 1 h with or without 5 μM cucurbitacin I (Merck) before metalloprotoporphyrin treatment. BMDC maturation was initiated with 500 ng/ml LPS (Sigma-Aldrich) for 24 h. Cells and supernatants were recovered for further analysis.

### *Coculture of BMDCs and $CD4^+$ T cells*

BMDCs ($4 \times 10^4$) were cultured in flat-bottom 96-well plates and treated as described above. After LPS treatment for 24 h, BMDCs were cocultured with $4 \times 10^5$ CFSE-labeled (Invitrogen) allogeneic $CD4^+$ T cells (either BALB/c or C57BL/6). Alloproliferation was measured after 5 days by flow cytometry (32).

### *Western blotting*

Western blotting was performed under standard conditions. In brief, $7.5 \times 10^5$ BMDCs were harvested, lysed, subjected to SDS-PAGE and transferred to nitrocellulose membranes (Hybond; Amersham Biosciences). Membranes were blocked with 5% nonfat dried milk in TBST (15 mM Tris-HCl (pH 8.0), 150 mM NaCl, and 0.1% Tween 20) and probed with primary Abs including anti-HO-1 (Nventa Biopharmaceuticals), anti-STAT3 (Cell Signaling Technology), anti-p38 MAPK (Cell Signaling), anti-Akt-1 (BD Biosciences), anti-phospho-STAT3 (BD Biosciences), anti-phospho-p38 MAPK (BD Biosciences), anti-phospho-Akt (BD Biosciences), anti-phospho-SAPK/JNK (where SAPK is stress-activated protein kinase; Cell Signaling), and anti-phospho-Erk1/2 (Cell Signaling) according to the manufacturer's instructions. Immunoreactive bands were detected using HRP-linked Abs against rabbit or mouse IgG (GE Healthcare) and Amersham ECL plus Western blotting detection system (GE Healthcare) according to the manufacturer's instructions.

### *Cytokine measurement*

Murine BMDCs were treated as described above and supernatants were collected for cytokine measurement applying BD Cytometric Bead Array analysis (BD Biosciences).

### *Flow cytometry*

Murine BMDCs were stained with biotinylated anti-MHC class II/PE-Cy5 coupled streptavidin and anti-CD86-FITC mAbs. PE-Cy5- or FITC-coupled rat anti-IgG2a κ isotypes were used as negative controls (all Abs were purchased from eBioscience). Measurements were performed using a FACSCalibur flow cytometer (BD Biosciences). Data analysis was performed using Summit version 3.1 software (Cytomation).

### *Statistical analysis*

Statistical analysis was performed using the nonparametric exact Mann-Whitney *U* test for small sample cohorts. All tests were assessed two-tailed using SPSS software version 12, and a probability of $p < 0.05$ was considered significant.

## Results

### *CoPPIX induces STAT3 in vivo*

The biostatistical cluster analysis of gene expression profiles generated from murine whole liver tissues (C57BL/6) revealed a clear induction of STAT3 and SOCS3 exclusively following

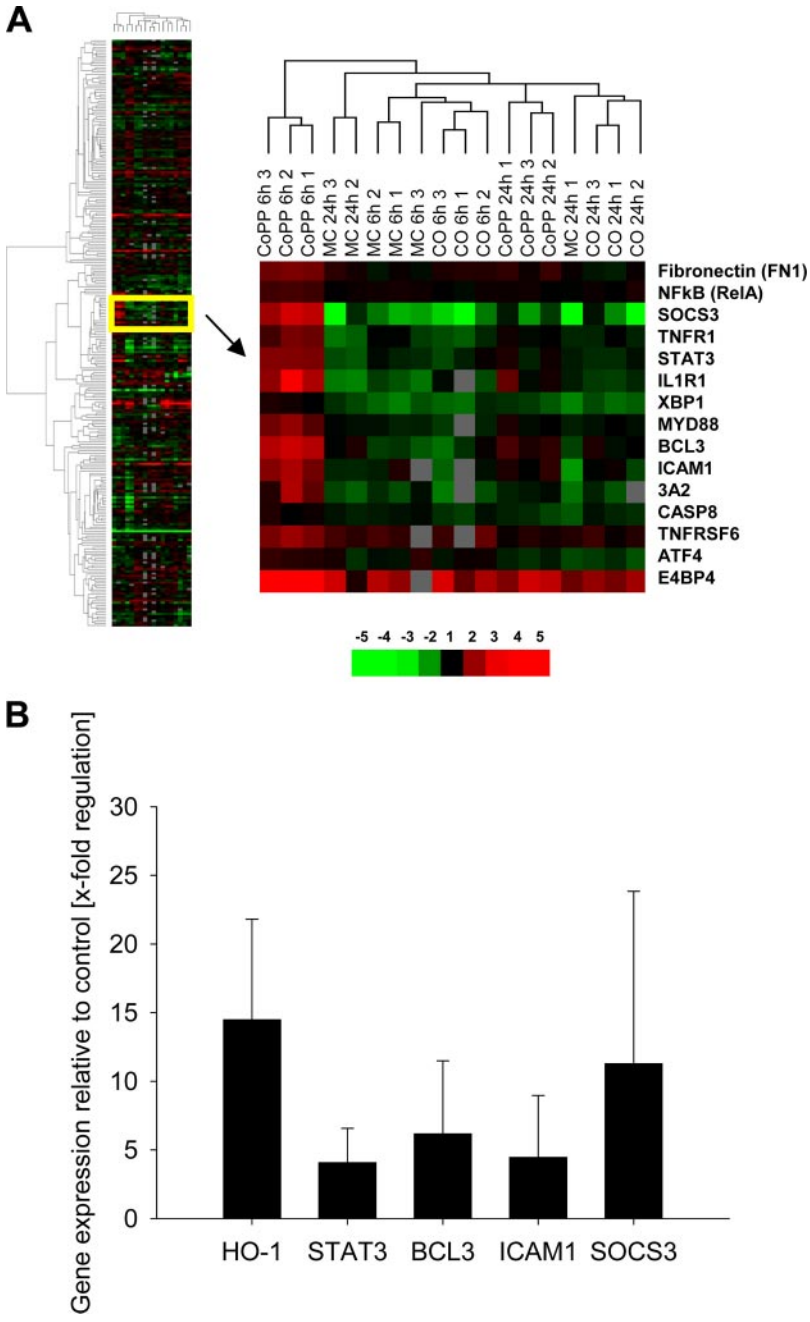


**FIGURE 1.** STAT3 is exclusively induced following CoPPIX treatment. *A*, Gene expression dendrogram showing hierarchical clustering of genes detectable in at least 80% of all cDNA microarray experiments performed. A short treatment with CoPPIX (CoPP) (6 h) resulted in a clear induction of a set of genes including *STAT3*, *SOCS3*, *BCL3*, *ICAM-1*, *TNFR1*, and *IL1R1*. *B*, RT-PCR analysis of an independent experiment using animals treated with CoPPIX ($n = 3$) or PBS ($n = 3$). The relative gene expression levels of *STAT3*, *SOCS3*, *BCL3*, *ICAM-1*, and *HO-1* after CoPPIX treatment were comparable to expression levels gained from the cDNA microarray experiment (mean expression level of 3 independent experiments is shown).

6 h of CoPPIX treatment (Fig. 1*A*). In addition to *STAT3* and *SOCS3*, genes including *B cell lymphoma 3* (*BCL3*), ICAM-1, *TNFR1*, and *IL1R1* were also up-regulated upon 6 h of CoPPIX treatment and clustered in close vicinity to *STAT3* and *SOCS3*, indicating that 6 h of treatment with CoPPIX was clearly different from all other types of conditioning (Fig. 1*A*). Gene expression of *STAT3* and *SOCS3* was additionally verified by real-time RT-PCR (data not shown). To confirm the data observed with the cDNA microarray, we performed an independent experiment by treating animals with CoPPIX ($n = 3$). We confirmed the gene expression of *STAT3* and *SOCS3* and additionally of *BCL3*, *ICAM-1*, and *HO-1* as a control for the presence of CoPPIX in the liver by real-time RT-PCR. The analysis revealed an induction of all genes with expression levels comparable to those observed in the cDNA microarray experiment (Fig. 1*B*).

*Knockdown of STAT3 and HO-1 in BMDCs*

The maturation process of BMDCs has been shown to be inhibited by STAT3 activation (24) and HO-1 induction (12). Furthermore the up-regulation of HO-1 by IL-10 was demonstrated to be partly mediated by STAT3 (33). To investigate the functional role of STAT3 and HO-1 in BMDC maturation, we designed siRNA against STAT3 (siSTAT3) and HO-1 (siHO-1) and confirmed effective knockdown of protein expression by Western blot analysis. Compared with n.s. siRNA, pretreated BMDCs, siSTAT3 resulted in a strong reduction of STAT3 total protein after IL-10 treatment. Additionally we demonstrated that the IL-10-mediated HO-1 expression is attenuated in the absence of STAT3 (Fig. 2*A*). Because IL-10 is a strong activator of STAT3, we achieved a strong phosphorylation in BMDCs within 15 min following treatment. In immature BMDCs transfected with siSTAT3, IL-10-mediated STAT3 phosphorylation was diminished

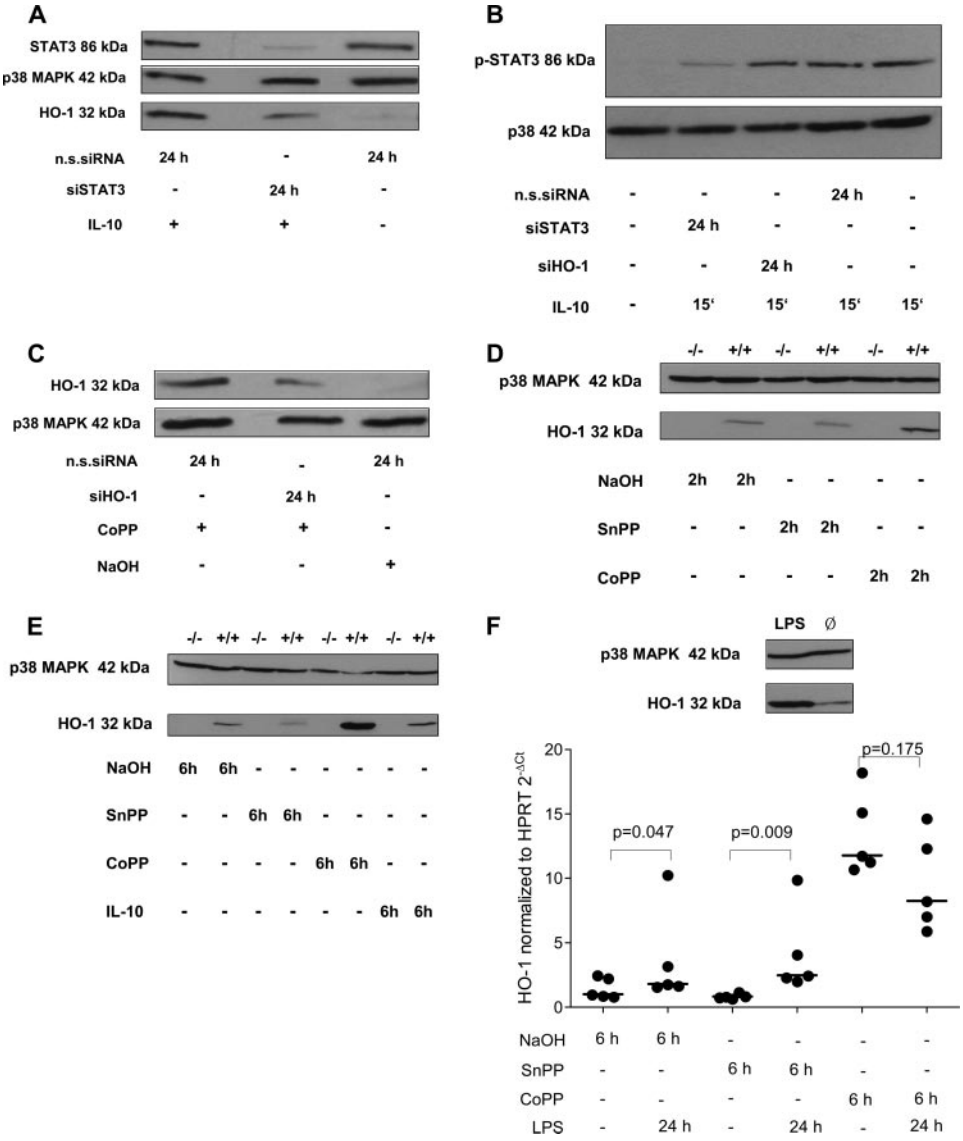


**FIGURE 2.** Protein expression of STAT3 and HO-1 in BMDCs from HO-1 knockout and wild-type mice. *A*, Analysis by Western blotting illustrated the specific siRNA-mediated knockdown of STAT3 in immature BMDCs. Compared with n.s. siRNA-pretreated BMDCs, STAT3 knockdown attenuated IL-10-mediated HO-1 expression. *B*, IL-10 treatment in immature BMDCs led to STAT3 phosphorylation (p-STAT3) within 15 min (15′) that was specifically blocked in the presence of siSTAT3. *C*, Western blot analysis demonstrating that transfection of BMDCs with siHO-1 results in reduced HO-1 protein levels after CoPPIX treatment. *D* and *E*, HO-1 protein expression was only detectable and induced in BMDCs derived from wild-type animals following 2 and 6 h of CoPPIX (CoPP) or SnPPIX (SnPP) treatment (*D*) and following 6 h of IL-10 treatment (*E*). *F*, LPS treatment for 24 h resulted in clear HO-1 expression in BMDCs as illustrated at the protein and mRNA levels. Significant induced HO-1 mRNA expression was observed in LPS-matured wild-type BMDCs pretreated with NaOH or SnPPIX ($p < 0.05$ and $p < 0.01$), whereas CoPPIX-pretreated BMDCs showed elevated HO-1 levels independently of LPS treatment ($n = 5$, mean ± SD). For Western blot analysis the same cell number ($1 \times 10^6$ BMDCs) and protein amount (100 $\mu$g) were used. An Ab directed against total p38 MAPK was used as loading control. The expression of total p38 MAPK was not influenced by the metalloporphyrin or by LPS or IL-10, as illustrated. One representative example from three experiments is shown for all Western blot data in this figure.

(Fig. 2*B*), thus demonstrating the efficiency of the applied siRNA. Correspondingly, siHO-1 pretreatment resulted in reduced protein levels after CoPPIX-mediated HO-1 induction (Fig. 2*C*).

### *CoPPIX induces HO-1 in BMDCs*

It has been reported that HO-1 induction after CoPPIX treatment of immature BMDCs is able to up-regulate and inhibit LPS-mediated DC maturation (12). To further evaluate this observation, we used BMDCs generated from HO-$1^{-/-}$ knockout and wild-type animals to examine the functional role of HO-1 in the BMDC maturation process by analyzing HO-1 protein expression after CoPPIX, SnPPIX, and IL-10 treatment. As expected, HO-1 was only induced in immature BMDCs from wild-type mice following 2 and 6 h of CoPPIX treatment, and HO-1 protein was further detected in wild-type BMDCs treated with SnPPIX or IL-10 induction (Fig. 2, *D* and *E*). To determine whether mature BMDCs lose their ability to express HO-1, we matured wild-type mouse-derived BMDCs with LPS treatment for 24 h and compared the HO-1 protein expression level to that of immature BMDCs. In contrast to previous observations (12), HO-1 expression is induced after LPS-dependent maturation and results were further confirmed at the mRNA level (Fig. 2*F*).

### *CoPPIX inhibits the maturation of HO-$1^{-/-}$ BMDCs*

To further determine the involvement of HO-1 expression in the maturation process of BMDCs, we generated DCs from HO-$1^{-/-}$

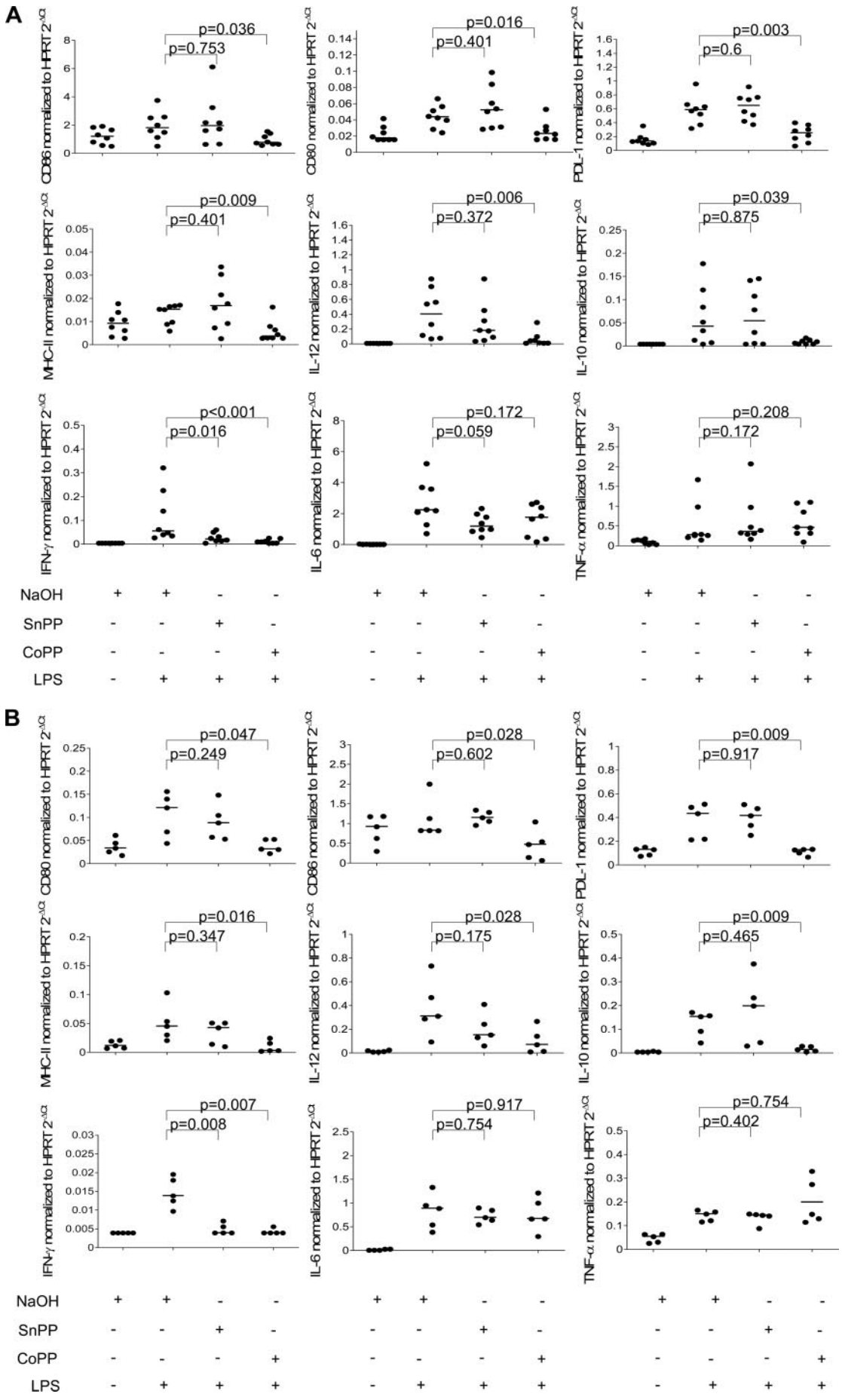

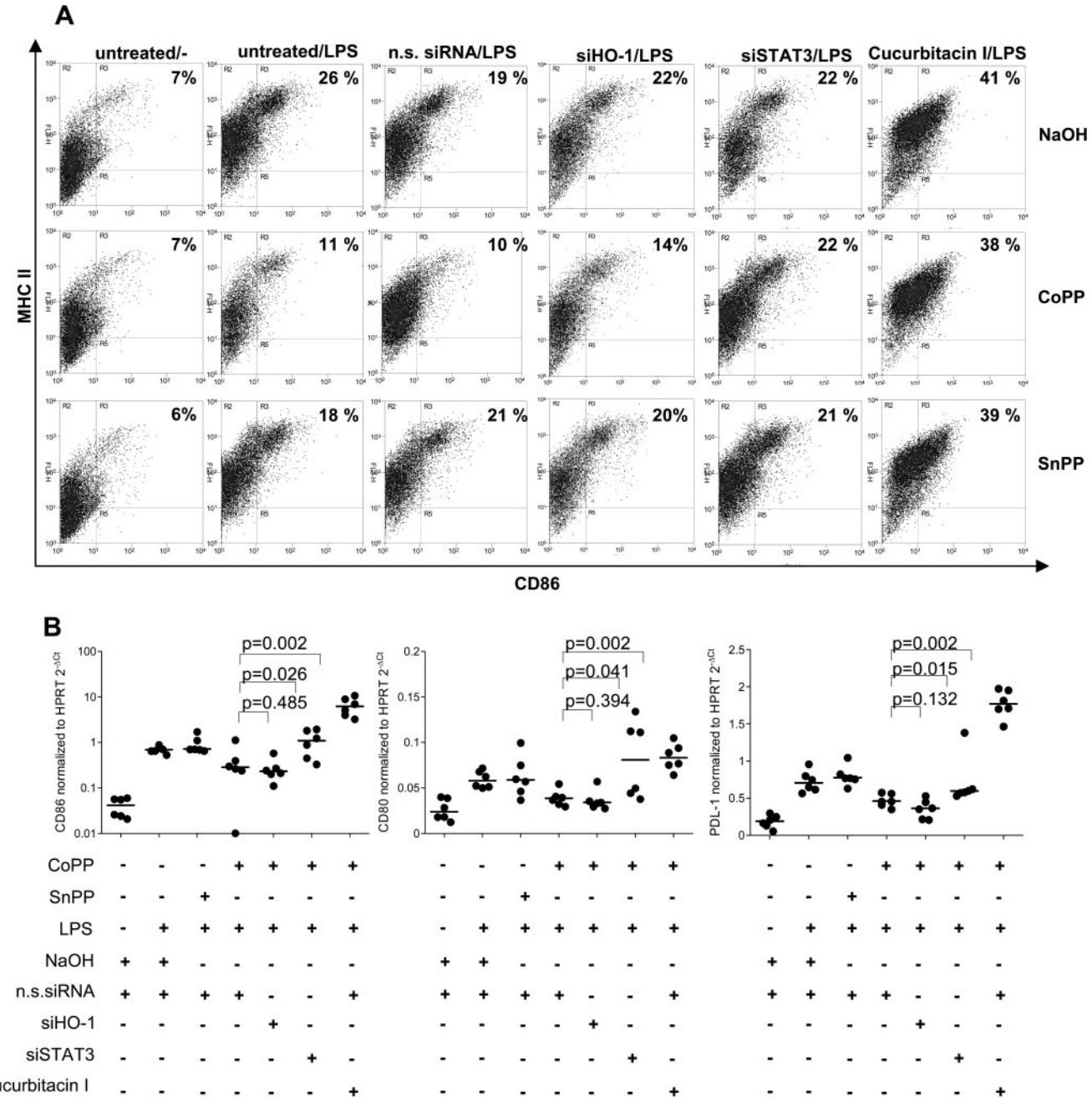


**FIGURE 4.** CoPPIX inhibits the LPS-mediated maturation of BMDCs independently of HO-1. *A*, Flow cytometric analysis illustrating the phenotype of BMDCs treated or untreated with CoPPIX (CoPP), SnPPIX (SnPP), or NaOH and matured with LPS (one representative example from three independent experiments is shown). BMDCs upon CoPPIX treatment showed a significant reduction in the coexpression of MHC class II and CD86 compared with SnPPIX- or NaOH-treated controls. Specific knockdown of STAT3 by siRNA reversed the reduction of MHC class II and CD86 double-positive BMDCs after CoPPIX treatment. The inhibitory effect of CoPPIX on BMDC maturation, characterized by the percentage of MHC class II/CD86 double-positive cells after LPS treatment of BMDCs, was significantly blocked with the STAT3 phosphorylation inhibitor cucurbitacin I. The CoPPIX-mediated inhibitory effect on LPS-induced BMDC maturation was not abolished by siHO-1. *B*, Reduction of *PDL-1*, *CD80*, and *CD86* mRNA expression was observed after CoPPIX treatment compared with NaOH- or SnPPIX-pretreated LPS-matured BMDCs. This inhibitory effect on gene expression was reversed by siSTAT3 or cucurbitacin I but was not affected by the application of siHO-1 ($n = 6$; significance was assessed by Mann-Whitney *U* test).

and wild-type mice. Cells were also exposed to CoPPIX and SnPPIX and maturation was induced by LPS. In general, the results shown in Fig. 3 demonstrate similar expression patterns in BMDCs generated from HO-$1^{-/-}$ mice (Fig. 3*A*) and those generated from wild-type mice (Fig. 3*B*). The LPS-mediated induction of surface markers, including *CD80/86*, *PDL-1*, *MHC class II*, and

**FIGURE 3.** RT-PCR analysis of candidate markers in HO-$1^{-/-}$-derived BMDCs ($n = 8$) (*A*) or wild-type-derived BMDCs ($n = 5$) (*B*) treated with either SnPPIX (SnPP), CoPPIX (CoPP), or NaOH for 6 h, cultured for a further 2 h, and left untreated or matured for 24 h with LPS. Induction of the surface markers *CD80*, *CD86*, *PDL-1*, and *MHC class II*, and the cytokines IL-10 and IL-12 following LPS treatment was significantly diminished by CoPPIX but was not altered by SnPPIX. Pretreatment of BMDCs with CoPPIX or SnPPIX had no effect on *TNF-α* or *IL-6* expression. LPS-induced *IFN-γ* was significantly reduced after both CoPPIX and SnPPIX treatment in HO-$1^{-/-}$ and wild-type BMDCs (significance was assessed by Mann-Whitney *U* test).

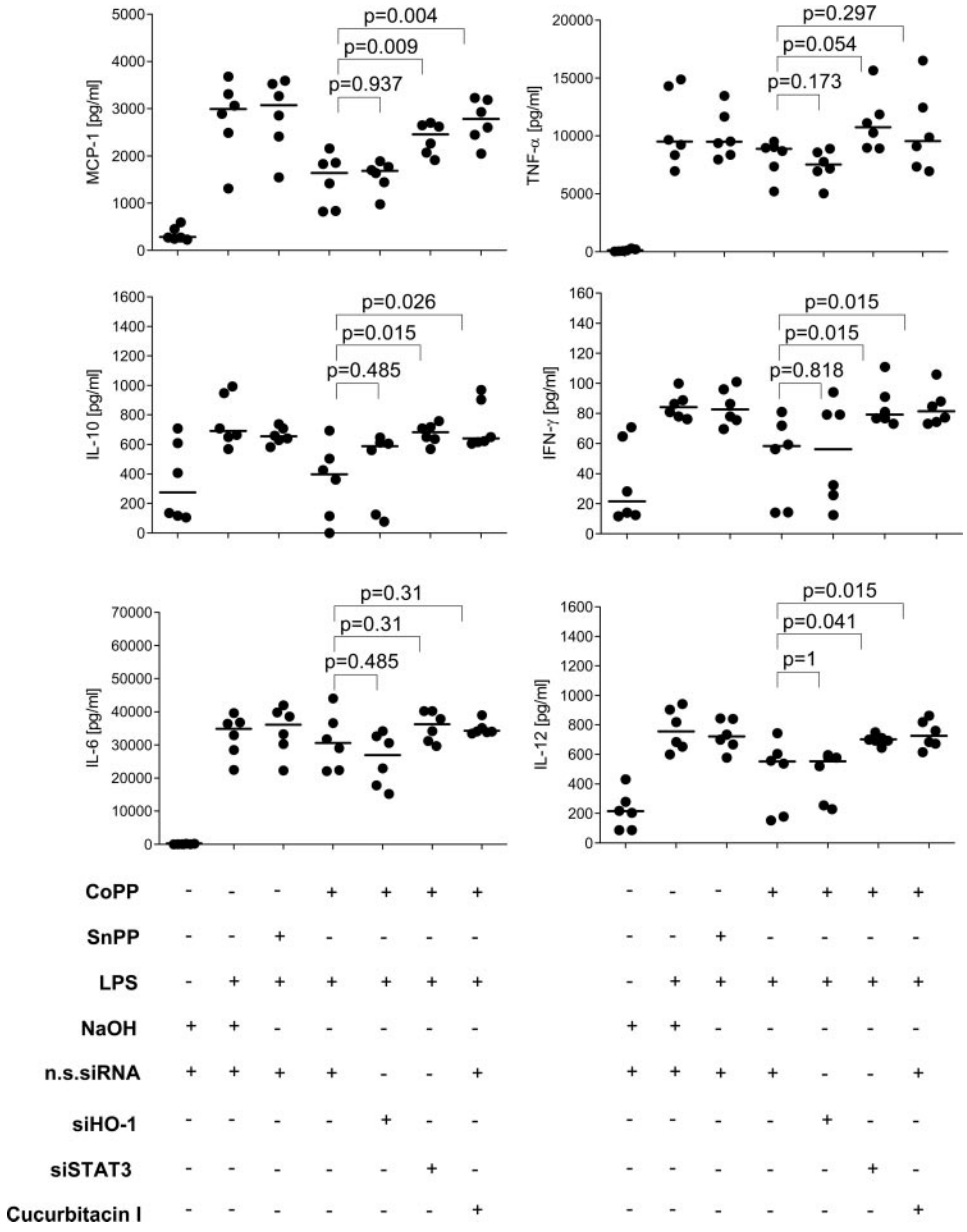


**FIGURE 5.** CoPPIX-mediated inhibition of the LPS-induced cytokine secretion in BMDCs requires STAT3 and is independent of HO-1. Reduction of IL-10, IL-12, MCP-1, and IFN-γ was observed after CoPPIX (CoPP) treatment compared with NaOH- and SnPPIX (SnPP)-pretreated LPS-matured BMDCs. This inhibitory effect on cytokine secretion was significantly reversed by the application of siSTAT3 or cucurbitacin I. Use of siHO-1 did not affect the inhibitory effect on cytokine secretion. Secretion of IL-6 and TNF-α was not altered by CoPPIX ($n = 6$, significance was assessed by Mann-Whitney *U* test).

cytokine genes including *IL-10* and *IL-12*, was significantly diminished after CoPPIX treatment but was not altered by SnPPIX in both groups (Fig. 3). Pretreatment of BMDCs with CoPPIX or SnPPIX had no effect on *TNF-α* and *IL-6* expression. The expression of *IFN-γ*, which was induced as a consequence of LPS treatment, was significantly reduced with CoPPIX and SnPPIX in both wild-type and knockout mice (Fig. 3). Interestingly, in agreement with other reports we observed significantly increased levels of inflammatory cytokine genes, including *IL-6*, *TNF-α*, and *IFN-γ* ($p \leq 0.05$) in LPS-matured BMDCs derived from HO-$1^{-/-}$ mice compared with wild-type mice (25, 34, 35) (data not shown).

### *STAT3 is required for inhibition of BMDC maturation*

Our cDNA microarray results illustrated an involvement of STAT3 following CoPPIX-mediated HO-1 induction. Therefore, we investigated whether there is a relationship between CoPPIX-induced inhibition of BMDC maturation by LPS and the transcription factor STAT3. CoPPIX pretreatment of immature DCs before LPS maturation led to a significant decrease of MHC class II and CD86 double-positive cells compared with DCs that remained untreated (10.7 ± 2.9% vs 22.8 ± 2.2%; $p < 0.001$, median ± mean deviation) (Fig. 4*A* and data not shown). However, specific knockdown using siSTAT3 significantly reversed the reduction of MHC class II and CD86 double-positive BMDCs (17.2 ± 1.4% vs 10.7 ± 2.9%, $p < 0.001$) (Fig. 4*A* and data not shown). To further confirm the functional involvement of STAT3 in inhibiting BMDC maturation, we used cucurbitacin I as a chemical inhibitor of STAT3 activation (36). Pretreatment of immature DCs with cucurbitacin I enhanced the maturation of BMDCs caused by LPS. Similar to the use of siRNA against STAT3, cucurbitacin I arrested the inhibitory effect of CoPPIX on LPS-induced BMDC maturation (33.3 ± 6.6% vs 37.6 ± 5.4%, $p = 0.161$) (Fig. 4*A* and data not shown). To verify whether HO-1 is responsible for the CoPPIX-mediated inhibition of LPS-induced DC maturation (12) we applied siHO-1. In contrast to previous observations, we did not observe any interference of CoPPIX-mediated inhibitory effects on LPS-induced BMDC maturation characterized by MHC class II and CD86 double-positive cells in DCs transfected with siHO-1 compared with the DCs transfected with n.s. siRNA (11.2 ± 3.2% vs 10.7 ± 2.9%, $p$ = NS) (Fig. 4*A* and data not

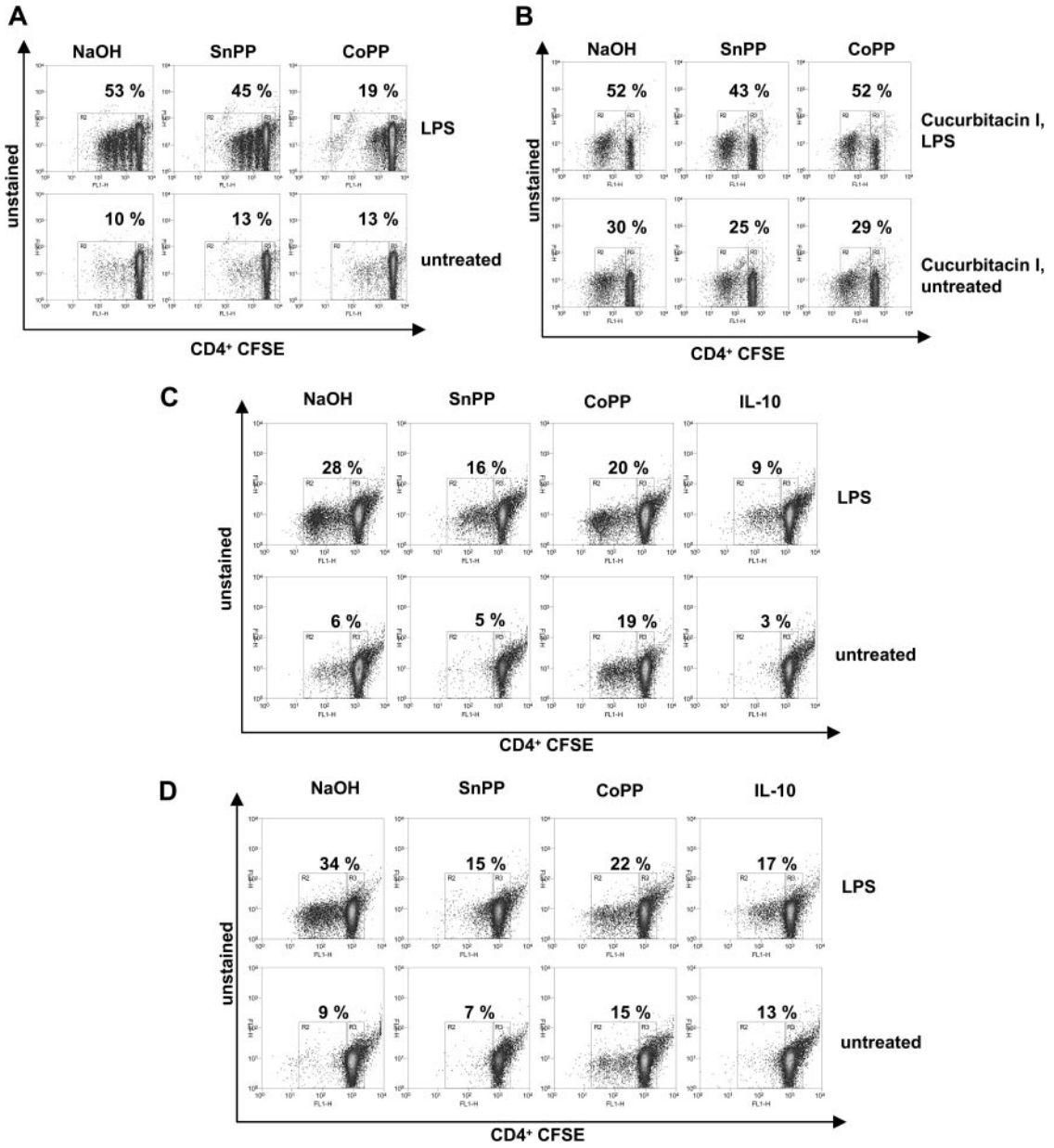


**FIGURE 6.** STAT3-dependent and HO-1-independent inhibition of $CD4^+$ T cell alloproliferation by CoPPIX (CoPP)- and SnPPIX (SnPP)-pretreated matured BMDCs. *A*, Flow cytometric analysis illustrating the diminished alloproliferation of C57BL/6 $CD4^+$ T cells coincubated with BMDCs generated from BALB/c mice following 6 h of CoPPIX pretreatment. SnPPIX had a moderate inhibitory effect on alloproliferation of $CD4^+$ T cells. *B*, Pretreatment of BMDCs with cucurbitacin I caused a high $CD4^+$ T cell alloproliferation. Blockade of the STAT3 signaling pathway before CoPPIX treatment in BMDCs abolished the inhibitory effect on T cell proliferation. *C*, C57BL/6 × FVB BMDCs from HO-1 knockout mice were pretreated with CoPPIX, SnPPIX, and IL-10 for 6 h following LPS treatment for 24 h. Inhibitory effects of pretreated and LPS-matured BMDCs on BALB/c-derived $CD4^+$ T cell alloproliferation were observed for CoPPIX, SnPPIX, and IL-10. *D*, BMDCs derived from wild-type animals treated with CoPPIX, SnPPIX, and IL-10 show inhibitory effects on alloproliferation similar to those observed for HO-$1^{-/-}$-derived BMDCs (data are representative of three independent experiments).

shown). Additionally we measured the mRNA expression of BMDC maturation markers, including PDL-1, CD80, and CD86, by real-time RT-PCR. The mRNA expression of CD80/86 and PDL-1 showed a reduction in CoPPIX-pretreated and LPS-matured BMDCs, and this effect was reversed by siSTAT3 ($p = 0.026$) and cucurbitacin I ($p = 0.002$) but was not influenced by siHO-1 ($p$ = NS) (Fig. 4*B*). We further determined the secretion of cytokines, including MCP-1, IL-6, IL-10, IL-12, TNF-$\alpha$, and IFN-$\gamma$. The results gained with LPS-matured BMDCs demonstrated a clear reduction of IL-10 ($p < 0.05$), IL-12 ($p < 0.05$), MCP-1 ($p < 0.05$), and IFN-$\gamma$ after CoPPIX ($p < 0.05$) treatment compared with NaOH or SnPPIX treatment, whereas the secretion of IL-6 and TNF-$\alpha$ was not altered by CoPPIX. This inhibitory effect on cytokine secretion was significantly reversed by siSTAT3 (IL-10, $p = 0.015$; IL-12, $p = 0.041$; MCP-1, $p = 0.009$; IFN-$\gamma$, $p = 0.015$) or inhibition of STAT3 (IL-10, $p = 0.026$; IL-12, $p = 0.015$; MCP-1, $p = 0.004$; IFN-$\gamma$, $p = 0.015$) action. In contrast the use of siHO-1 did not affect the inhibitory effect on cytokine secretion ($p$ = NS) (Fig. 5).

Next, we determined the ability of the BMDCs to initiate the alloproliferation of $CD4^+$ T cells and tested whether DCs in a less mature state due to CoPPIX pretreatment were able to attenuate the proliferation of alloreactive T cells. As shown in Fig. 6*A*, alloproliferation of C57BL/6 $CD4^+$ T cells was diminished as a

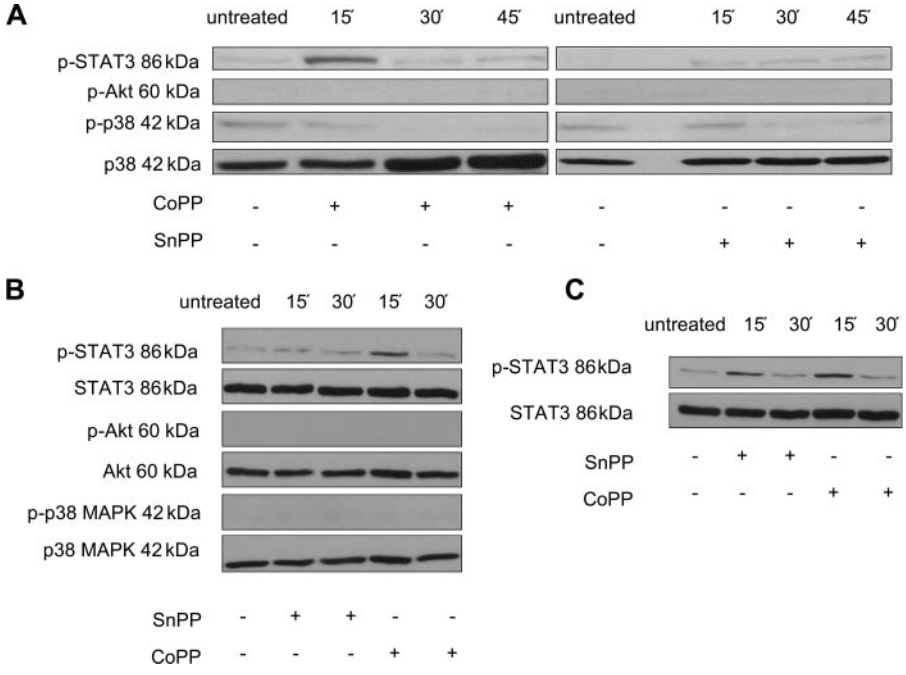


**FIGURE 7.** CoPPIX leads to STAT3 activation in immature BMDCs. *A*, Western blot analysis showing an activation of STAT3 after 15 min of CoPPIX (CoPP) treatment in immature BMDCs. Application of SnPPIX (SnPP) also demonstrated a weak activation of STAT3. The PI3K pathway represented by Akt phosphorylation and the p38 MAPK pathway were not activated by CoPPIX or by SnPPIX. *B*, Activation of STAT3 after 15 min of CoPPIX treatment of HO-$1^{-/-}$-derived immature BMDCs. No Akt phosphorylation or p38 MAPK pathway activation was observed. *C*, Phosphorylation of STAT3 (p-STAT3) in C57BL/6 × FVB BMDCs after CoPPIX pretreatment. SnPPIX also led to activation of STAT3, although to a lesser extent compared with CoPPIX (one representative example from at least three independent experiments is shown).

consequence of the CoPPIX pretreatment of BMDCs generated from BALB/c mice. Interestingly, SnPPIX also had a moderate inhibitory effect on $CD4^+$ T cell alloproliferation (Fig. 6*A*). Immature BMDCs pretreated with cucurbitacin I caused a high alloproliferation rate when not matured with LPS (Fig. 6*B*). In addition, the blockade of the STAT3 signaling pathway by cucurbitacin I before CoPPIX treatment and LPS-induced DC maturation interrupted any inhibitory effect on alloproliferation (Fig. 6*B*). We generated BMDCs from HO-1 knockout and wild-type animals and in both of these an inhibitory effect of CoPPIX-, SnPPIX-, and IL-10-pretreated and LPS-matured BMDCs on $CD4^+$ T cell alloproliferation (BALB/c) was observed (Fig. 6, *C* and *D*). Immature DCs treated with IL-10 before LPS-induced DC maturation were very potent in inhibiting proliferation of $CD4^+$ T cells independently of HO-1 expression (Fig. 6, *C* and D). Together with IL-10 as a native activator of the STAT3 signaling pathway and DCs generated from HO-$1^{-/-}$ mice, we corroborated our results illustrating the importance of STAT3 mediating the inhibitory capacity of CoPPIX on DC maturation independently of HO-1 activity.

### *CoPPIX leads to STAT3 phosphorylation*

Knowing the importance of STAT3 in mediating the inhibitory effect on LPS-induced DC maturation, we investigated the ability of CoPPIX or SnPPIX to modulate different signaling pathways, including the p38 MAPK, PI3K, STAT3, ERK, and JNK pathways. We analyzed activation profiles in the early phase after the treatment of immature BMDCs to ensure that activation was caused by CoPPIX alone and was not due to HO-1 activity. First we demonstrated a phosphorylation of STAT3 15 min after CoPPIX treatment on BMDCs. SnPPIX also had a weak activation effect on STAT3 (Fig. 7*A*). The PI3K pathway represented by Akt phosphorylation and the p38 MAPK pathway were not initiated by CoPPIX or SnPPIX (Fig. 7*A*). The same results were gained with BMDCs generated from HO-$1^{-/-}$ and wild-type mice (Fig. 7, *B* and *C*, and data not shown). In addition, we examined the phosphorylation status of ERK1/2 and JNK1/2/3 in HO-$1^{-/-}$ and wild-type BMDCs. Within the short incubation time period of up to 30 min we were not able to detect any phosphorylation for either pathway analyzed (data not shown). These data demonstrate an initiation of STAT3 signaling for both CoPPIX and SnPPIX with different intensities independent of HO-1 activity.

## Discussion

In extensive experimental studies, treatment of donor allografts with the metalloporphyrin CoPPIX to induce HO-1 has been proven to ameliorate I/R injury (16–18, 20, 21). In this context it is assumed that the inhibitory effect of HO-1 induction after CoPPIX application on DC maturation might provide an explanation for the better graft outcome posttransplantation (20, 23). In contrast to previous observations (12, 13), our data show that the CoPPIX-induced inhibition of LPS-mediated BMDC maturation is dependent on STAT3 phosphorylation but independent of HO-1. Using cDNA microarrays we demonstrated that a short treatment of mice with CoPPIX (6 h) resulted in a clear induction of STAT3 and SOCS3 in the liver (Fig. 1*A*). The induction of SOCS3 as a surrogate marker for STAT3 activation (37) was accompanied by the expression of additional genes, including BCL3 and ICAM-1, which are also known to be induced upon STAT3 activation (Fig. 1*B*) (38, 39). STAT3 is phosphorylated within 15 min following CoPPIX treatment (Fig. 7 and data not shown). The decreased phenotypic maturation state characterized by reduced levels of CD80/86, PDL-1, MHC class II, MCP-1, IL-12, IL-10, and IFN-γ following CoPPIX application was reversed by inhibiting STAT3 expression or activation through the application of siRNA or cucurbitacin I, a substance that inhibits STAT3 phosphorylation and promotes the activation of immature DCs (Figs. 4 and 5) (40). CoPPIX-mediated inhibition of LPS-induced DC maturation was not abolished using BMDCs derived from HO-$1^{-/-}$ mice, corroborating our findings that HO-1 activity is not the main mechanism of DC maturation (Fig. 3). Analysis of the phenotype of matured BMDCs derived from HO-$1^{-/-}$ and wild-type mice reveals a similar gene expression pattern for DC maturation-associated markers independent of HO-1 expression (Fig. 3).

Interestingly we were not able to observe a preservation of IL-10 in BMDCs pretreated with CoPPIX compared with previous observations in rat BMDCs and in human monocyte-derived DCs (12). In contrast, we observed a decrease in IL-10 production after 2 h and diminished levels of IL-10 mRNA expression after 6 h of

CoPPIX pretreatment in LPS-matured BMDCs. Similar effects were reported from mixed lymphocyte reactions by Woo et al., where a decrease in lymphoproliferation and IL-10 and IFN-$\gamma$ production was detected as an effect of CoPPIX pretreatment (18). The observed discrepancies with previous reports concerning the preservation of IL-10 production or LPS-induced HO-1 induction in BMDCs might be attributable to species-specific differences (12, 13). However, the observation that LPS strongly induces HO-1 was made not only in murine but also in rat BMDCs (23).

Furthermore we analyzed the alloproliferation of BALB/c $CD4^+$ T cells mixed with C57BL/6 $\times$ FVB HO-$1^{-/-}$ and wild-type-derived BMDCs. Consistent with the results from coculture experiments with BALB/c BMDCs and C57BL/6 $CD4^+$ T cells, we observed a reduction of alloproliferation with CoPPIX, SnPPIX, and IL-10 compared with BMDCs pretreated with NaOH (Fig. 6). Surprisingly, although we could detect no inhibitory effect of SnPPIX on the phenotype of mature BMDCs, SnPPIX pretreatment of BMDCs seemed to have a greater inhibitory effect on $CD4^+$ T cell proliferation compared with that of CoPPIX (Fig. 6*A*). Nevertheless, subtracting the spontaneous alloproliferation rate caused by pretreated immature BMDCs showed that CoPPIX pretreatment was still more effective than SnPPIX pretreatment. The different maximum alloproliferation rates obtained for coculture experiments, including those involving BALB/c-derived BMDCs and C57BL/6 $CD4^+$ T cells (Fig. 6, *A* and *B*) and C57BL/6 $\times$ FVB HO-$1^{-/-}$ and wild-type-derived BMDCs and BALB/c $CD4^+$ T cells (Fig. 6, *C* and *D*), can be explained by the different genetic backgrounds of the $CD4^+$ T cells. It is well known that BALB/c mice produce Th type 2 responses and fail to promote cellular Th1 responses to infection (41). This biological attribute is manifested by a lower maximum alloproliferation rate in BALB/c $CD4^+$ T cells when cocultured with C57BL/6 $\times$ FVB HO-$1^{-/-}$ and wild-type-derived BMDCs (Fig. 6, *C* and *D*). However, more evidence indicating that HO-1 is not involved in the process of LPS-induced BMDC maturation is provided by using SnPPIX as a competitive inhibitor of HO-1 (11). We demonstrated that SnPPIX itself shows inhibitory capacity (Fig. 6) and leads to enhanced HO-1 levels in LPS-matured BMDCs (Fig. 2*F*). The ability of CoPPIX-pretreated and LPS-matured DCs to inhibit allogeneic $CD4^+$ T cell proliferation was abolished by cucurbitacin I (Fig. 6*B*). Interestingly, IL-10 pretreatment of LPS-matured BMDCs was very potent in inhibiting alloproliferation of $CD4^+$ T cells independently of HO-1 expression (Fig. 6, *C* and *D*). Consistent with the findings of Ricchetti et al. (33), we demonstrated that the induction of HO-1 by IL-10 is in part mediated by STAT3 but, in contrast to other observations (42), the anti-inflammatory effect of IL-10 could not be attributed to HO-1 expression by using knockout mice.

The activation of STAT3 signaling with tumor-derived factors such as vascular-endothelial-growth-factor (VEGF) or IL-10 has been shown to negatively regulate DC maturation, whereas blocking of STAT3 abolished this inhibitory effect (43). Furthermore Corinti et al. demonstrated that, in contrast to mature DCs, immature DCs readily activate STAT3 upon IL-10 treatment, suggesting a mechanism by which IL-10 could limit LPS-mediated DC maturation (44). We observed an activation of STAT3 upon CoPPIX treatment of immature DCs that was more efficient than the activation achieved with SnPPIX treatment. Besides the PI3K pathway, the three major MAPK pathways p38, ERK, and JNK were not activated by CoPPIX, suggesting a central role for STAT3 in mediating the inhibitory effect of CoPPIX on LPS-induced BMDC maturation (Fig. 7). Moreover, activation of STAT3 seemed not to be dependent on the autocrine secretion of IL-10 or IL-6, as CoPPIX was still able to inhibit LPS-induced DC maturation in the presence of IL-10- and IL-6-neutralizing Abs (data not shown). Given that STAT3 is reported to be activated in cells by ROS (45–47), we hypothesize that the CoPPIX-mediated activation of STAT3 is due to the modulation of the redox state within the cell. Furthermore, a phosphorylation-independent homodimerization of STAT3 upon oxidative stress was demonstrated by Li and Shaw (48). CoPPIX has been shown to cause a decrease in LPS-induced ROS production in rat BMDCs (12), thus altering the cellular redox state. Although this effect has been ascribed to the antioxidative activity of HO-1, we speculate that CoPPIX mediates an alteration of the cellular redox state by inhibiting microsomal enzymes including cytochrome P-450 (49) and NADPH cytochrome P-450 reductase (50) independently of HO-1 induction. Inhibition of cytochrome P-450 reductase has been also reported for SnPPIX (51), which also might have an impact on STAT3 activation. Although not proven, this potential activation of STAT3 might explain the capacity of SnPPIX-pretreated BMDCs to inhibit T cell alloproliferation (Fig. 6).

The anti-inflammatory and cell-protective effects of HO-1 and its degradation products have been proven in many experimental models (15). Recently, Zhang et al. demonstrated the activation of STAT3 upon overexpression of HO-1 in murine lung endothelial cells (MLEC) (52). They also correlated protection against hyperoxia-induced cell death with the activation of STAT3, which confers MLEC protection via both HO-1-dependent and -independent mechanisms. The present study demonstrates that the inhibitory effects of CoPPIX on LPS-induced murine BMDC maturation is mediated by STAT3 and is independent of HO-1. Furthermore, our data show an elevation of HO-1 expression in LPS-induced mature BMDCs. Although induction of HO-1 in BMDCs by IL-10 was in part mediated by the expression of STAT3, we demonstrated that the anti-inflammatory effect of IL-10 did not require the expression of HO-1. These findings might lead to a better understanding of how CoPPIX in part mediates protection against I/R injury as reported in the literature (16–21, 23). The identification of STAT3 as a downstream effector of CoPPIX provides a molecular target in DCs for the generation of Ag-specific immune tolerance, with profound implications for transplantation medicine.

## Acknowledgments

We thank Dr. Anupam Agarwal, University of Alabama, for providing the HO-$1^{-/-}$ mice.

## Disclosures

The authors have no financial conflict of interest.

## References

1. Fossiez, F., O. Djossou, P. Chomarat, L. Flores-Romo, S. Ait-Yahia, C. Maat, J. J. Pin, P. Garrone, E. Garcia, S. Saeland, et al. 1996. T cell interleukin-17 induces stromal cells to produce proinflammatory and hematopoietic cytokines. *J. Exp. Med.* 183: 2593–2603.
2. Adema, G. J., F. Hartgers, R. Verstraten, E. de Vries, G. Marland, S. Menon, J. Foster, Y. Xu, P. Nooyen, T. McClanahan, et al. 1997. A dendritic-cell-derived C-C chemokine that preferentially attracts naive T cells. *Nature* 387: 713–717.
3. Morelli, A. E., and A. W. Thomson. 2003. Dendritic cells: regulators of alloimmunity and opportunities for tolerance induction. *Immunol. Rev.* 196: 125–146.
4. Larsen, C. P., P. J. Morris, and J. M. Austyn. 1990. Migration of dendritic leukocytes from cardiac allografts into host spleens: a novel pathway for initiation of rejection. *J. Exp. Med.* 171: 307–314.
5. Saiki, T., T. Ezaki, M. Ogawa, and K. Matsuno. 2001. Trafficking of host- and donor-derived dendritic cells in rat cardiac transplantation: allosensitization in the spleen and hepatic nodes. *Transplantation* 71: 1806–1815.
6. Hamrah, P., S. O. Huq, Y. Liu, Q. Zhang, and M. R. Dana. 2003. Corneal immunity is mediated by heterogeneous population of antigen-presenting cells. *J. Leukocyte Biol.* 74: 172–178.
7. Chiang, Y. J., L. Lu, J. J. Fung, and S. Qian. 2001. Liver-derived dendritic cells induce donor-specific hyporesponsiveness: use of sponge implant as a cell transplant model. *Cell Transplant.* 10: 343–350.
8. Morelli, A. E., P. J. O'Connell, A. Khanna, A. J. Logar, L. Lu, and A. W. Thomson. 2000. Preferential induction of Th1 responses by functionally

mature hepatic ($CD8\alpha^-$ and $CD8\alpha^+$) dendritic cells: association with conversion from liver transplant tolerance to acute rejection. *Transplantation* 69: 2647–2657.
9. Steptoe, R. J., F. Fu, W. Li, M. L. Drakes, L. Lu, A. J. Demetris, S. Qian, H. J. McKenna, and A. W. Thomson. 1997. Augmentation of dendritic cells in murine organ donors by Flt3 ligand alters the balance between transplant tolerance and immunity. *J. Immunol.* 159: 5483–5491.
10. Jiang, S., O. Herrera, and R. I. Lechler. 2004. New spectrum of allorecognition pathways: implications for graft rejection and transplantation tolerance. *Curr. Opin. Immunol.* 16: 550–557.
11. Kappas, A., and G. S. Drummond. 1986. Control of heme metabolism with synthetic metalloporphyrins. *J. Clin. Invest.* 77: 335–339.
12. Chauveau, C., S. Remy, P. J. Royer, M. Hill, S. Tanguy-Royer, F. X. Hubert, L. Tesson, R. Brion, G. Beriou, M. Gregoire, et al. 2005. Heme oxygenase-1 expression inhibits dendritic cell maturation and proinflammatory function but conserves IL-10 expression. *Blood* 106: 1694–1702.
13. Listopad, J., K. Asadullah, C. Sievers, T. Ritter, C. Meisel, R. Sabat, and W. D. Docke. 2007. Heme oxygenase-1 inhibits T cell-dependent skin inflammation and differentiation and function of antigen-presenting cells. *Exp. Dermatol.* 16: 661–670.
14. Tenhunen, R., H. S. Marver, and R. Schmid. 1968. The enzymatic conversion of heme to bilirubin by microsomal heme oxygenase. *Proc. Natl. Acad. Sci. USA* 61: 748–755.
15. Ryter, S. W., J. Alam, and A. M. Choi. 2006. Heme oxygenase-1/carbon monoxide: from basic science to therapeutic applications. *Physiol. Rev.* 86: 583–650.
16. Tullius, S. G., M. Nieminen-Kelha, R. Buelow, A. Reutzel-Selke, P. N. Martins, J. Pratschke, U. Bachmann, M. Lehmann, D. Southard, S. Iyer, et al. 2002. Inhibition of ischemia/reperfusion injury and chronic graft deterioration by a single-donor treatment with cobalt-protoporphyrin for the induction of heme oxygenase-1. *Transplantation* 74: 591–598.
17. Kotsch, K., M. Francuski, A. Pascher, R. Klemz, M. Seifert, J. Mittler, G. Schumacher, R. Buelow, H. D. Volk, S. G. Tullius, et al. 2006. Improved long-term graft survival after HO-1 induction in brain-dead donors. *Am. J. Transplant.* 6: 477–486.
18. Woo, J., S. Iyer, M. C. Cornejo, N. Mori, L. Gao, I. Sipos, M. Maines, and R. Buelow. 1998. Stress protein-induced immunosuppression: inhibition of cellular immune effector functions following overexpression of haem oxygenase (HSP 32). *Transpl. Immunol.* 6: 84–93.
19. Gerbitz, A., P. Ewing, A. Wilke, T. Schubert, G. Eissner, B. Dietl, R. Andreesen, K. R. Cooke, and E. Holler. 2004. Induction of heme oxygenase-1 before conditioning results in improved survival and reduced graft-versus-host disease after experimental allogeneic bone marrow transplantation. *Biol. Blood Marrow Transplant.* 10: 461–472.
20. Martins, P. N., H. Kessler, A. Jurisch, A. Reutzel-Selke, J. Kramer, A. Pascher, J. Pratschke, P. Neuhaus, H. D. Volk, and S. G. Tullius. 2005. Induction of heme oxygenase-1 in the donor reduces graft immunogenicity. *Transplant. Proc.* 37: 384–386.
21. Kato, H., F. Amersi, R. Buelow, J. Melinek, A. J. Coito, B. Ke, R. W. Busuttil, and J. W. Kupiec-Weglinski. 2001. Heme oxygenase-1 overexpression protects rat livers from ischemia/reperfusion injury with extended cold preservation. *Am. J. Transplant.* 1: 121–128.
22. Martins, P. N., A. Reutzel-Selke, A. Jurisch, C. Denecke, K. Attrot, A. Pascher, K. Kotsch, J. Pratschke, P. Neuhaus, H. D. Volk, and S. G. Tullius. 2006. Induction of carbon monoxide in donor animals prior to organ procurement reduces graft immunogenicity and inhibits chronic allograft dysfunction. *Transplantation* 82: 938–944.
23. Kotsch, K., P. N. Martins, R. Klemz, U. Janssen, B. Gerstmayer, A. Dernier, A. Reutzel-Selke, U. Kuckelkorn, S. G. Tullius, and H. D. Volk. 2007. Heme oxygenase-1 ameliorates ischemia/reperfusion injury by targeting dendritic cell maturation and migration. *Antioxid. Redox. Signal.* 9: 2049–2063.
24. Park, S. J., T. Nakagawa, H. Kitamura, T. Atsumi, H. Kamon, S. Sawa, D. Kamimura, N. Ueda, Y. Iwakura, K. Ishihara, et al. 2004. IL-6 regulates in vivo dendritic cell differentiation through STAT3 activation. *J. Immunol.* 173: 3844–3854.
25. Kapturczak, M. H., C. Wasserfall, T. Brusko, M. Campbell-Thompson, T. M. Ellis, M. A. Atkinson, and A. Agarwal. 2004. Heme oxygenase-1 modulates early inflammatory responses: evidence from the heme oxygenase-1-deficient mouse. *Am. J. Pathol.* 165: 1045–1053.
26. Kotsch, K., M. F. Mashreghi, G. Bold, P. Tretow, J. Beyer, M. Matz, J. Hoerstrup, J. Pratschke, R. Ding, M. Suthanthiran, et al. 2004. Enhanced granulysin mRNA expression in urinary sediment in early and delayed acute renal allograft rejection. *Transplantation* 77: 1866–1875.
27. Bosio, A., C. Knorr, U. Janssen, S. Gebel, H. J. Haussmann, and T. Muller. 2002. Kinetics of gene expression profiling in Swiss 3T3 cells exposed to aqueous extracts of cigarette smoke. *Carcinogenesis* 23: 741–748.
28. Weiss, S., K. Kotsch, M. Francuski, A. Reutzel-Selke, L. Mantouvalou, R. Klemz, O. Kuecuek, S. Jonas, C. Wesslau, F. Ulrich, et al. 2007. Brain death activates donor organs and is associated with a worse I/R injury after liver transplantation. *Am. J. Transplant.* 7: 1584–1593.
29. Inaba, K., M. Inaba, N. Romani, H. Aya, M. Deguchi, S. Ikehara, S. Muramatsu, and R. M. Steinman. 1992. Generation of large numbers of dendritic cells from mouse bone marrow cultures supplemented with granulocyte/macrophage colony-stimulating factor. *J. Exp. Med.* 176: 1693–1702.
30. Yuan, B., R. Latek, M. Hossbach, T. Tuschl, and F. Lewitter. 2004. siRNA selection server: an automated siRNA oligonucleotide prediction server. *Nucleic Acids Res.* 32: W130–W134.
31. Zhang, X., P. Shan, D. Jiang, P. W. Noble, N. G. Abraham, A. Kappas, and P. J. Lee. 2004. Small interfering RNA targeting heme oxygenase-1 enhances ischemia-reperfusion-induced lung apoptosis. *J. Biol. Chem.* 279: 10677–10684.
32. Lyons, A. B., and C. R. Parish. 1994. Determination of lymphocyte division by flow cytometry. *J. Immunol. Methods* 171: 131–137.
33. Ricchetti, G. A., L. M. Williams, and B. M. Foxwell. 2004. Heme oxygenase 1 expression induced by IL-10 requires STAT-3 and phosphoinositol-3 kinase and is inhibited by lipopolysaccharide. *J. Leukocyte Biol.* 76: 719–726.
34. Poss, K. D., and S. Tonegawa. 1997. Heme oxygenase 1 is required for mammalian iron reutilization. *Proc. Natl. Acad. Sci. USA* 94: 10919–10924.
35. Poss, K. D., and S. Tonegawa. 1997. Reduced stress defense in heme oxygenase 1-deficient cells. *Proc. Natl. Acad. Sci. USA* 94: 10925–10930.
36. Blaskovich, M. A., J. Sun, A. Cantor, J. Turkson, R. Jove, and S. M. Sebti. 2003. Discovery of JSI-124 (cucurbitacin I), a selective Janus kinase/signal transducer and activator of transcription 3 signaling pathway inhibitor with potent antitumor activity against human and murine cancer cells in mice. *Cancer Res.* 63: 1270–1279.
37. Kubo, M., T. Hanada, and A. Yoshimura. 2003. Suppressors of cytokine signaling and immunity. *Nat. Immunol.* 4: 1169–1176.
38. Brocke-Heidrich, K., B. Ge, H. Cvijic, G. Pfeifer, D. Loffler, C. Henze, T. W. McKeithan, and F. Horn. 2006. BCL3 is induced by IL-6 via Stat3 binding to intronic enhancer HS4 and represses its own transcription. *Oncogene* 25: 7297–7304.
39. Wooten, D. K., X. Xie, D. Bartos, R. A. Busche, G. D. Longmore, and S. S. Watowich. 2000. Cytokine signaling through Stat3 activates integrins, promotes adhesion, and induces growth arrest in the myeloid cell line 32D. *J. Biol. Chem.* 275: 26566–26575.
40. Nefedova, Y., P. Cheng, D. Gilkes, M. Blaskovich, A. A. Beg, S. M. Sebti, and D. I. Gabrilovich. 2005. Activation of dendritic cells via inhibition of Jak2/STAT3 signaling. *J. Immunol.* 175: 4338–4346.
41. Guler, M. L., J. D. Gorham, C. S. Hsieh, A. J. Mackey, R. G. Steen, W. F. Dietrich, and K. M. Murphy. 1996. Genetic susceptibility to *Leishmania*: IL-12 responsiveness in TH1 cell development. *Science* 271: 984–987.
42. Lee, T. S., and L. Y. Chau. 2002. Heme oxygenase-1 mediates the anti-inflammatory effect of interleukin-10 in mice. *Nat. Med.* 8: 240–246.
43. Wang, T., G. Niu, M. Kortylewski, L. Burdelya, K. Shain, S. Zhang, R. Bhattacharya, D. Gabrilovich, R. Heller, D. Coppola, et al. 2004. Regulation of the innate and adaptive immune responses by Stat-3 signaling in tumor cells. *Nat. Med.* 10: 48–54.
44. Corinti, S., C. Albanesi, A. la Sala, S. Pastore, and G. Girolomoni. 2001. Regulatory activity of autocrine IL-10 on dendritic cell functions. *J. Immunol.* 166: 4312–4318.
45. Liu, T., S. Castro, A. R. Brasier, M. Jamaluddin, R. P. Garofalo, and A. Casola. 2004. Reactive oxygen species mediate virus-induced STAT activation: role of tyrosine phosphatases. *J. Biol. Chem.* 279: 2461–2469.
46. Carballo, M., M. Conde, R. El Bekay, J. Martin-Nieto, M. J. Camacho, J. Monteseirin, J. Conde, F. J. Bedoya, and F. Sobrino. 1999. Oxidative stress triggers STAT3 tyrosine phosphorylation and nuclear translocation in human lymphocytes. *J. Biol. Chem.* 274: 17580–17586.
47. Simon, A. R., U. Rai, B. L. Fanburg, and B. H. Cochran. 1998. Activation of the JAK-STAT pathway by reactive oxygen species. *Am. J. Physiol.* 275: C1640–C1652.
48. Li, L., and P. E. Shaw. 2004. A STAT3 dimer formed by inter-chain disulphide bridging during oxidative stress. *Biochem. Biophys. Res. Commun.* 322: 1005–1011.
49. Spaethe, S. M., and D. J. Jollow. 1989. Effect of cobalt protoporphyrin on hepatic drug-metabolizing enzymes: specificity for cytochrome P-450. *Biochem. Pharmacol.* 38: 2027–2038.
50. Yanni, S. B., J. P. Chism, D. E. Rickert, and C. J. Serabjit-Singh. 1993. Diminished drug metabolism due to hormonal effects of cobalt mesoporphyrin on flavoproteins. *Chem. Biol. Interact.* 89: 73–87.
51. Maines, M. D., and G. M. Trakshel. 1992. Tin-protoporphyrin: a potent inhibitor of hemoprotein-dependent steroidogenesis in rat adrenals and testes. *J. Pharmacol. Exp. Ther.* 260: 909–916.
52. Zhang, X., P. Shan, G. Jiang, S. S. Zhang, L. E. Otterbein, X. Y. Fu, and P. J. Lee. 2006. Endothelial STAT3 is essential for the protective effects of HO-1 in oxidant-induced lung injury. *FASEB J.* 20: 2156–2158.